AD-A063 596 CASE WESTERN RESERVE UNIV CLEVELAND OHIO DEPT OF MACR--ETC F/G 20/11
ON THE MECHANISM OF PRESSURE-INDUCED ENVIRONMENTAL STRESS CRACK--ETC(U)
DEC 78 A MOET, E BAER N00014-75-C-0795
UNCLASSIFIED TR-7 NL

1 OF 1
AD A063596

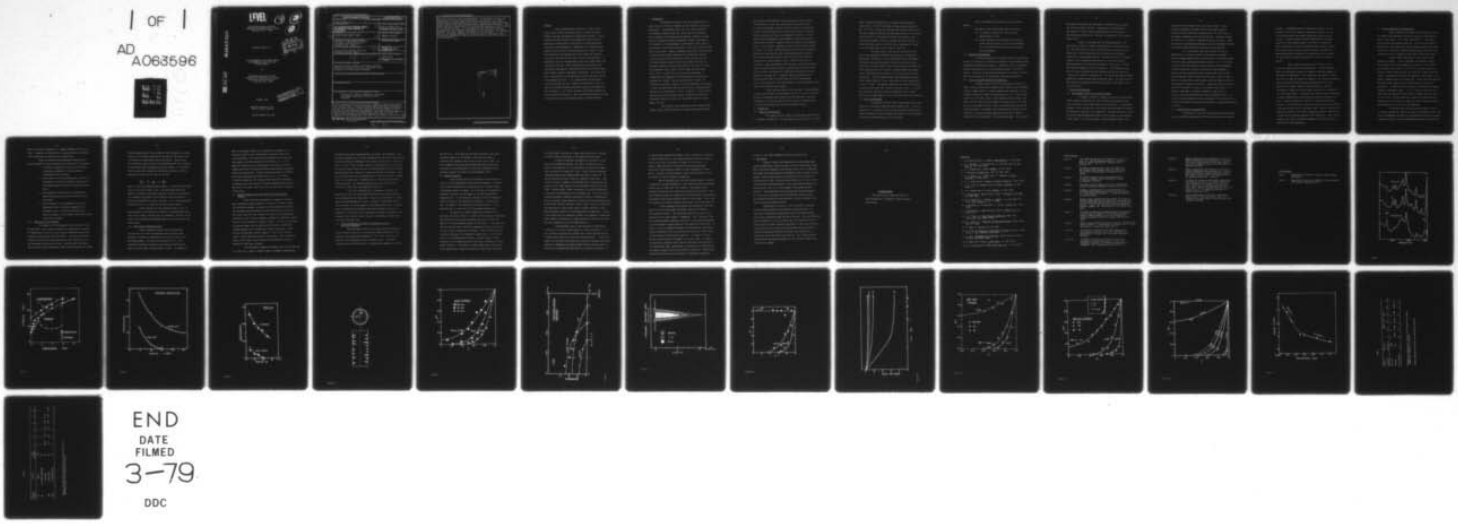

END
DATE FILMED
3-79
DDC

CASE WESTERN RESERVE UNIVERSITY
Department of Macromolecular Science
Cleveland, Ohio 44106

Technical Report No. 7

ON THE MECHANISM OF PRESSURE-INDUCED ENVIRONMENTAL STRESS CRACKING IN POLYSTYRENE

by

Abdelsamie Moet and Eric Baer
Department of Macromolecular Science
Case Western Reserve University
Cleveland, Ohio 44106

December 1978

Research Sponsored by the
Office of Naval Research

Contract N00014-75-C-0795

SECURITY CLASSIFICATION OF THIS PAGE *(When Data Entered)*

REPORT DOCUMENTATION PAGE

READ INSTRUCTIONS BEFORE COMPLETING FORM

1. REPORT NUMBER: Technical Report #7
2. GOVT ACCESSION NO.:
3. RECIPIENT'S CATALOG NUMBER:

4. TITLE *(and Subtitle)*: ON THE MECHANISM OF PRESSURE-INDUCED ENVIRONMENTAL STRESS CRACKING IN POLYSTYRENE.

5. TYPE OF REPORT & PERIOD COVERED: Technical Report, Interim

6. PERFORMING ORG. REPORT NUMBER:

7. AUTHOR(s): Abdelsamie Moet and Eric Baer

8. CONTRACT OR GRANT NUMBER(s): N00014-75-C-0795

9. PERFORMING ORGANIZATION NAME AND ADDRESS:
Department of Macromolecular Science
Case Western Reserve University
Cleveland, Ohio 44106

10. PROGRAM ELEMENT, PROJECT, TASK AREA & WORK UNIT NUMBERS:

11. CONTROLLING OFFICE NAME AND ADDRESS:
Office of Naval Research (Code 472)
Arlington, Virginia 22217

12. REPORT DATE: December 22, 1978

13. NUMBER OF PAGES: 42p.

14. MONITORING AGENCY NAME & ADDRESS *(if different from Controlling Office)*: TR-7

15. SECURITY CLASS. *(of this report)*: Unclassified

15a. DECLASSIFICATION/DOWNGRADING SCHEDULE:

16. DISTRIBUTION STATEMENT *(of this Report)*

Approved for public release; distribution unlimited.
Reproduction in whole or in part is permitted for any purpose of the United States Government.

17. DISTRIBUTION STATEMENT *(of the abstract entered in Block 20, if different from Report)*

18. SUPPLEMENTARY NOTES

19. KEY WORDS *(Continue on reverse side if necessary and identify by block number)*

High pressure, Tension, Compression, Polystyrene, Environment, Penetration, Infra-red, Craze, Transition

20. ABSTRACT *(Continue on reverse side if necessary and identify by block number)*

Fluids conventionally classified as "inert" exerted a strong stress crazing and cracking effect on certain amorphous polymers when they are deformed in tension under pressure. Fourier transform infrared difference spectroscopy has been utilized to measure the concentration of trace amounts of fluid penetrating the polymer during deformation. Measurable fluid penetration was found to take place only in dilated structures as large as crazes. The penetration level depended upon craze density and structure, viscosity of the

DD FORM 1 JAN 73 1473 EDITION OF 1 NOV 65 IS OBSOLETE
S/N 0102-014-6601

SECURITY CLASSIFICATION OF THIS PAGE *(When Data Entered)*

408 357 LB

fluid and the time or rate of the experiment. At atmospheric pressure, the penetrating fluid front lagged behind the dry growing craze tip. Radial concentration distributions were successfully described by a semiquantitative porous transport model which yielded a specific penetration coefficient. This coefficient was a strong function of the hydrostatic pressure and the viscosity of the penetrating fluid. It is suggested that the hydrostatic pressure decreases the "void" content in the polymeric solid, yet due to the pressure gradient concurrently enhances the dynamics of fluid transport. At a critical pressure, the polymer undergoes the brittle-to-ductile transition. Here irreversible deformation by shear is preferred over the void forming craze or cracking mechanism.

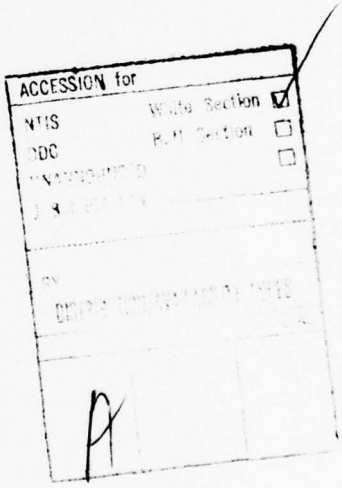

Synopsis

Fluids conventionally classified as "inert" exert a strong stress crazing and cracking effect on certain amorphous polymers when they are deformed in tension under pressure. Fourier transform infrared difference spectroscopy has been utilized to measure the concentration of trace amounts of fluid penetrating the polymer during deformation. Measurable fluid penetration was found to take place only in dilated structures as large as crazes. The penetration level depended upon craze density and structure, viscosity of the fluid and the time or rate of the experiment. At atmospheric pressure, the penetrating fluid front lagged behind the dry growing craze tip. Radial concentration distributions were successfully described by a semiquantitative porous transport model which yielded a specific penetration coefficient. This coefficient was a strong function of the hydrostatic pressure and the viscosity of the penetrating fluid. It is suggested that the hydrostatic pressure decreases the "void" content in the polymeric solid, yet due to the pressure gradient concurrently enhances the dynamics of fluid transport. At a critical pressure, the polymer undergoes the brittle-to-ductile transition. Here irreversible deformation by shear is preferred over the void forming craze or cracking mechanism.

1. Introduction

The behavior of polymers under the combined effect of stress and active fluid environments has been intensively studied in recent years. Environmental stress crazing is usually observed with amorphous polymers below their glass transition temperature and is believed to be enhanced by the presence of swelling liquids. Based on different experimental approaches, several investigators [1-4] agreed that the enhancement of environmental effect seems to be maximized if the solubility parameter of the liquid closely matches that of the polymer. However, subsequent experiments with wide range of polymer-liquid systems suggested that correlation of solvent crazing with solubility parameter was found to be very poor [5]. A fracture mechanics approach [2,6] has concluded that both the threshhold conditions and the growth kinetics for cracks or crazes are governed by stress intensity factor rather than by overall stress [4,7], or strain [1] as was previously maintained. A related study [8] suggested the minimun surface work required to propagate the 'starter' crack as an alternative criteria. An indisputable conclusion, however, is that environmental craze growth is fluid flow-controlled under various conditions although detailed modeling of the flow kinetics is still in question. Fluid viscosity and wetting ability have been briefly, though not systematically, considered as possible criteria for the determination of environmental activity.

Most previous investigations have been conducted under simple uniaxial tensile loading, to elucidate the mechanism and/or

the mechanics of environmental effects caused by "active" fluids. Little attention, if any, has been paid to the possible effects of "inert" environments, especially when the system is subjected to a stress field more complex than simple uniaxial tension. Thus far, fluids have been classified as environmentally "active" or "inert" based on their enhancement of environmental crazing and cracking in simple uniaxial tension. Recently, Baer and coworkers [9] discovered that all liquids tested, regardless of their previous classification as "active" or "inert", exhibited marked stress cracking to polymers tested in uniaxial tension under superposed hydrostatic pressure. This alarming discovery questions the validity of the traditional classification of environmental fluids. While this work was in preparation , Ward and Coworkers [10] reported a similar environmental stress crazing and cracking effect in polycarbonate under the effect of pure torsion, and previously in PMMA under combined torsion and hydrostatic pressure [11]. It appears obvious, therefore, that the macroscopic stress field and localized stress concentration play a significant role in the determination of the environmental stress cracking of a polymer-liquid system.

In this paper we report a novel approach: the measurements of actual flow kinetics of environmental fluids (silicon oils) into the polymer (polystyrene) under different applied hydrostatic pressures. The mechanism of pressure-induced stress-crazing and cracking effect is explained using new model for the environmental process.

2. Experimental

2.1. Materials and specimens

The polymer used was commercial polystyrene supplied as 0.5 in. diameter extruded rod. All experiments were carried out on a single

batch of material characterized by a number average molecular weight of $\bar{M}_n = 1.05 \times 10^5$ and weight average molecular weight of $\bar{M}_w = 2.46 \times 10^5$. The tensile specimens were machined from the rods into the standard cylindrical type described in detail in a previous publication [12]. Also machined from the same rods were round compression specimens of 0.20 in. diameter and 0.60 in.height. A lathe machine was used to turn both kinds of specimens at a speed of 20 rpm taking cuts of 0.010 inches in the finish.

The gauge length of the tensile specimens and both ends of the compression specimens were polished by conventional metalographic techniques, first using WETODRY 600 SiC (3M Company) followed by emery polishing paper 2/0 and then with 0.3μm Al_2O_3 applied on a polishing cloth (Fisher microcloth) wet with distilled water ending up with 0.05 μm Al_2O_3. Polished samples were washed several times with distilled water in an ultrasonic bath at room temperature. Clean polished specimens were subsequently annealed at 86°C under vacuum for 50 hrs. then cooled to room temperature at a rate of 10°C/hr. The annealed specimens, which were individually examined by polarized light, showed no residual strains. To protect the compression specimen from the environmental fluid, a gold-pallidium coat about 200Å thi k was applied uniformly after annealing.

2.2. Tensile measurements

The apparatus used for tensile measurements under high hydrostatic pressure has been described elsewhere [13]. It consists essentially of a constant strain rate testing machine contained in a chamber filled with fluid to transmit the pressure. During specimen straining a constant pressure can be maintained.

Tests at atmospheric pressure were run in an Instron machine.

Two types of tensile experiments were carried out:

(1) To fracture in tension at a strain rate of approximately 1% / min.

(2) Stress relaxation; test specimens were strained to the required strain at a rate of approximately 10% / min and held at fixed strain for the period of the experiment.

2.3. Compression measurements

A device was designed for insertion into the high pressure machine which enabled us to measure the compressive yield behavior under superposed high hydrostatic pressure. Compression tests at atmospheric pressure were carried out in the conventional manner in an Instron machine. Two discs of poly(tetrafluoroethylene) of suitable size were used one at each end of the specimen for additional lubrication.

2.4. Fourier Transform Infrared (FTIR) Analysis

Specimens tested in the fluid environment (silicon oil) under various conditions were removed quickly from the test environment, carefully wiped, placed in a closed container then quenched in liquid nitrogen in order to "freeze" the constituents in situ. Using a lathe, radial layers of 0.005 inches in depth each were turned along a fixed height of 5/16 inches from the middle of the gauge length. The lathe was run at low speed (40 rpm) in order to minimize heating during the cutting procedure. Furthermore, the cutting tool was carefully wiped clean with a solvent and dried subsequent to each cut so that any transfer of oil from one shell to the next was avoided. The cut shells

were ground individually with KBr powder to prepare pellets suitable for FTIR spectroscopic analysis. Semiquantitative measurements of the amount of silicon oil which had penetrated into the specimen were achieved by application of the base line method to FTIR difference spectra [14].

Figure 1 illustrates the FTIR technique applied. The top spectra is that of a typical polystyrene shell containing silicon oil, the middle spectra is that of pure polystyrene standard and the bottom one is the difference spectra resulting from the automatic subtraction of the two upper spectra. The band 1260 cm^{-1} is of special interest in the semiquantitative analysis of silicon oil because polystyrene shows no significant absorbance in its vicinity. The 803 cm^{-1} band was frequently used for correlation. The absorbance of the 1260 cm^{-1} band calculated from the difference spectra was taken to be a function of silicon oil concentration. All subtractions were performed against one reference sample during the entire work. The sensitivity of this method was evaluated and found to be roughly in the order of one part per million.

3. Results and discussion

3.1. Environmental effects on yield and fracture

In figure 2, results of compressive yielding of polystyrene either exposed or protected from the environment are compared to the tensile behavior of the polymer under similar conditions. At atmospheric pressure, silicon oil had very little effect upon the mechanical behavior of polystyrene in tension or in compression. At higher pressures, silicon oil did not show any measurable effect on the compressive yield behavior of the polymer. In tension, however, protected samples showed slight

increase in their fracture stress up to about 0.3kbar. At this pressure polystyrene, protected from the environment, showed a brittle-to-ductile transition; and above which, the yield stress of the polymer increased with the applied pressure. Specimens exposed to silicon oil, in contrast, remained brittle up to 3.0kbar. Above this pressure, polystyrene became ductile and the environmental effect on the yield stress beyond this transition was not observed.

It is thus obvious that high viscosity silicon oil (500cSt) which is relatively inert to polystyrene at atmospheric pressure produced marked stress cracking effect to the polymer tested in tension under superposed hydrostatic pressure. It is of interest to add that Baer and coworkers [8] reported that other environments like water which has no effect on polystyrene under atmospheric pressure did cause pronounced stress cracking under high pressure. The environmental effect of water was found to be similar to that of methanol, a known stress cracking agent, under the combined effect of high hydrostatic pressure and tension. Polystyrene did not even show the ductile transition in water or in methanol up to 4.0kbar. It appears evident that a dilational component of the strain is a prerequisite for the manifestation of the environmental effect. This view was recently supported by Ward and coworkers [9] who reported on a similar environmental effect (with polycarbonate in diethyldihexylsebacate) in torsion.

3.2. Conditions for fluid penetration

Penetration of silicon oil (500cSt) into polystyrene under various conditions was measured by FTIR and the results are displayed

in table 1. Undeformed samples of polystyrene soaked in oil for 8 months (3.5×10^5 sec) showed no measurable sorption. Silicon oil did not penetrate into samples soaked under pressures up to 1.0kbars. In sharp contrast, when dry polystyrene was profusely crazed in air then soaked unloaded in silicon oil, penetration readily took place. The depth of penetration was found to increase with time and until a constant depth was reached. We have thus demonstrated that the formation of voided structures are required for the transport of measurable amounts of silicon oil into the polymer.

Table 2 shows the penetration of silicon oil into polystyrene under various loading conditions. Polymer maintained under pure hydrostatic pressure of 4.0kbar for two hours showed no measurable oil penetration. At 4.0 kbar,where polystyrene is known to be ductile, when the sample was exposed to 3.5% constant elongation, definite necking and shear banding were observed but no oil was detected at any depth. However, when subjected to 1% constant elongation at 1.0kbar the polymer showed crazing and oil penetration to a considerable depth. Furthermore, the fluid was found to penetrate at higher concentration uniformly when the sample was exposed to the same 1% constant elongation at 100 bars of superposed hydrostatic pressure. In this last case, crazing was observed to be more profusely spread along a wider span of the gauge length. Applying combined axial compressive strain of 3.0% under a superposed hydrostatic pressure of 100 bars did not show any measurable fluid penetration. These results suggest, again, that a dilational component of the applied stress is essential for fluid penetration.

3.3. Factors affecting fluid penetration

Figure 3 shows the concentration distribution of silicon oil (500cSt) into polystyrene fractured in tension at two different strain rates, namely, 2×10^{-3} min^{-1} and $10^{-4} min^{-1}$. Both samples were fractured under ambient conditions. Silicon oil was found to penetrate to a much higher level and to a greater depth at the lower strain rate. Although the penetration magnitude was different, the concentration profile appeared to be similar at both strain rates.

Figure 4 depicts the effect of strain level on the penetration kinetics. In this experiment, two identical samples were strained to two fixed elongations; 0.5% and 1% (in silicon oil at a constant strain rate of 2×10^{-2} min^{-1}), and kept loaded for one hour. Both of these strains fall within the "linear viscoelastic range" of polystyrene, well below the reported crazing strain for the specific geometery used in this work [12]. It was found that doubling the strain level caused some five fold increase in the level of penetration. In addition, the oil appears to have been driven deeper towards the specimen's center. It is of special interest to note that crazes were observed in both samples, however, they were scarce at 0.5% strain. As the samples were turned in the lathe machine in preparation of FTIR analysis, crazes were found to disappear around a depth beyond which no silicon oil was detected.

It has been shown that the amount and depth of silicon oil penetrating the test samples increased with decreasing strain rate. This rate dependency has been also concluded from previously reported experiments [9,10]. We further demonstrated here that the amount and

depth of silicon oil penetration is strongly dependent on the strain level. In general, the intensity of crazing was directly correlated with the magnitude of penetrating oil concentration.

Below are summarized the experimental observations of this environmental process according to the results thus far reported.

1. A dilational component of the strain (or stress) is a necessary requirement for pressure-induced environmental stress cracking.
2. Crazes form prior to fluid penetration and serve as the medium for silicon oil transport, especially in the apparent absence of molecular sorption of such a fluid.
3. High hydrostatic pressure alone or combined with nondilational strains can not drive the fluid into the polymer.
4. Fluid transport is a rate dependent process, the magnitude of which is strongly dependent on the dilational strain. At ambient conditions, the capillary pressure is high enough to drive the viscous fluid into the sample.

3.4.1. Modeling of Fluid Transport

The kinetics of fluid transport into the craze will now be considered. Since crazes are known to be highly porous structures, the penetration of silicon oil into crazes was modeled assuming fluid transport through porous capillary channels. The pressure difference between the fluid at the craze opening and at the growing craze tip was considered to be the driving force. Assuming that craze growth starts from the surface inwards and crazes are statistically distributed

along the gauge length of our cylinderical test specimen in a uniform fashion, as illustrated schematically in Figure 5, then Darcy's law for transport in porous media [15] can be applied. Starting from the differential form of Darcy's law, considering that fluid transport is every where radial and neglecting any end effects, it is possible [16,17] to derive an expression, describing the kinetics of fluid penetration suitable for our case, of the form

$$\frac{\partial C}{\partial t} = \frac{1}{r} \frac{\partial}{\partial r} \left(r \kappa \frac{\partial C}{\partial t} \right)$$

where C is the fluid concentration at radius r, r being the diminishing radius of dry core at time t, and κ the penetration coefficient. Numerical solutions of the above expression in terms of two dimentionless parameters (C/C_0) and (r/α) are given by Crank [17], where C is the fluid concentration at time t and radius r, C_0 is the extrapolated concentration at $r = \alpha$, α being the cylinder radius (Figure 5).

Similar analysis has been proposed by Barrer [16] as a possible means of the treatment of diffusion into heterogeneous media. Other forms of Darcy's law have been also adopted by Williams [2] and Kramer [6] to develop two independent models for fluid transport into single crazes.

3.4.2. Application to penetration data

Figure 6 represents typical radial concentration distributions of silicon oil penetrated into polystyrene under atmospheric pressure, as determined by FTIR analysis and fit into the proposed model. The solid lines represent the fit of the penetrability equation expressed in the previous section to data taken at various times of soaking under 1% strain. The numbers on

each curve represent values of the dimentionless parameter $\kappa t/\alpha^2$, from which values for the time-dependent penetration coefficient κ can be obtained. This coefficient was observed to increase with time towards a uniform concentration distribution, i.e., $\kappa t/\alpha^2=1$. Under this particular set of experimental conditions, $\kappa t/\alpha^2$ never reached unity prior to fracture time which occurred about 85 minutes after strain application. Instead, fracture occurred at $\kappa t/\alpha^2=0.08$, with approximate penetration coefficient of 3.6×10^{-7} cm^2/sec. It should be noted that the fracture time reported here represents an average value since fracture is strongly dependent upon the exact magnitude of the local strain as well as upon the specific nature of surface flaws.

3.5. Relation between craze front growth and fluid transport kinetics

Stress relaxation experiments at atmospheric pressure were performed on samples immersed in silicon oil in order to check the relationship between craze growth and fluid penetration kinetics. The experiments were performed for a definite period of time at the end of which the stress was released, but some of the specimens were maintained in their fluid environment, unloaded, for additional soaking. Results of this experiment is shown in Figure 7. Silicon oil was found to penetrate deeper into the specimen after one hour of additional unloaded soaking, that is without any further craze growth. After 24 hours of additional soaking, however, silicon oil was found to retract outward indicating possible craze healing. The craze healing effect is well known, since relatively high compressive forces are exerted on crazes upon unloading.

The relationship between the growing craze front and the flow of silicon oil is shown in figure 8, where a schematic representation

recreated from results shown graphically in figure 7 are displayed. The area AOB represents the fluid front as deduced from the initial concentration distribution measured immediately after soaking for one hour in silicon oil under 1% strain. After unloaded soaking of one additional hour, the fluid was found to spread further over an area represented by ECF which indicate deeper penetration by silicon oil without any possible craze growth. Thus the craze front must have had preceded the oil front by, at least, a length shown in the figure as OC. Unaccounted for is the craze healing effect discussed earlier. The same healing effect may also account for the closure with time of the craze opening from AB to EF.

It was thus concluded that, at atmospheric pressure, the penetrating silicon oil front lagged behind the growing craze front.This lag, represented by the distance OC in figure 8, was estimated to be about several hundred Angstroms per second. Although oil penetrated into the craze structure, it did not appear to have approached the tip, a condition which is believed to be inpoerative when high hydrostatic pressure is superposed. For the first time, experimental evidence is provided for the concept of "dry" tip for a "wet" craze, an idea previously communicated by Williams and Kramer [6].

3.6. Fluid viscosity and its effect on penetration kinetics and stress relaxation

Figure 9a depicts the radial concentration distributions of three different silicon oils of viscosities; 5000cSt, 500cSt and 1.5cSt, penetrated into polystyrene elongated to 1% for 1 hour, and figure 9b represents the corresponding stress relaxation curves. The stress cracking ability of the 1.5cSt oil, is stronger when compared to the other

two fluids [5]. This effect has also been reflected in the stress relaxation behavior of the polymer in the same fluid shown in figure 9b which reached as much as 70% of the initial stress. We wish to emphasize the close match between the shape of the radial distribution of the penetrated fluid and the corresponding stress relaxation behavior for each of the environmental fluids.

3.7. Effect of Pressure

Figure 10 shows the radial concentration distributions of silicon oil which penetrated into polystyrene extended to 1% tensile strain (stress relaxation) for varying periods of time while under a superposed pressure of 0.6kbar. As in the case of the behavior at atmospheric pressure, the data appear to fit the proposed model reasonably well. At this pressure, and again similar to atmospheric pressure (figure 6), the penetration coefficient κ increased with time. At 0.6kbar, $\kappa t/\alpha^2$ reached 0.25 in about two hours. It was estimated that in 3 hours the $\kappa t/\alpha^2$ value would approach unity.

The results of a similar experiments carried out at 0.9 and 1.2kbar are shown in figure 11. Again at this pressure, the proposed model continues to provide an acceptable description for the flow behavior of the environmental medium into the crazes. It has been also observed that the radial distribution changes more slowly with time at 0.9 and 1.2kbar in comparison with 0.6kbar. This can easily be noted by observing changes in the penetration coefficient, κ, at all pressures for corresponding time intervals. Pressure causes a marked reduction in fluid penetration due to the direct consequence of craze growth inhibition. This effect is further emphasized by noting that $\kappa t/\alpha^2$ reached unity in about 30 minutes at 0.1kbar (table 2) and was

less than 0.005 in one hour at 1.2kbar, thus amounting to a decrease in several orders of magnitude in the penetration coefficient.

In order to study more systematically the effect of pressure on the penetration behavior, the radial concentration distribution of the penetrant oil into the polymer was measured in samples which were held at 1% strain for 1 hour. Results of this experiment treated according to the proposed model are shown in figure 12. The applied pressures and $\kappa t/\alpha^2$ values are reported on each curve. From a value of unity at 0.2kbar, $\kappa t/\alpha^2$ decreased with increasing applied pressure up to 1.2kbar where $\kappa t/\alpha^2$ was estimated to be much less than 0.005. Therefore above 1.2kbar, the amount of fluid which penetrated is too small to be measured by this technique used. Since the analytic technique employed is capable of measuring silicon oil concentrations as low as one ppm, lesser amounts of silicon oil may have penetrated the polymer under strain at more than 1.2kbar. Indeed, this was indicated by the appearance of a few surface crazes in samples tested at 1.5kbar where meaningful analysis of fluid penetration was impossible. Inspite of the inability of our technique to detect trace amounts of penetration, some evidence of penetration at higher pressures and shorter test time has been presented in an earlier publication [9].

A semilogarithmic plot of the coefficient of penetration in one hour at 1% strain versus pressure is shown in figure 13. The data, falling on two distinct straight lines, reveal that the decrease in penetration coefficient follows two different regimes. In the first regime, the relatively high penetration coefficient dropped rapidly with pressure as compared to the second regime which was characterized by a slow decline in penetration coefficient as a function of pressure. It

is interesting to observe that regimes I and II intersect at a pressure of around 0.5kbar which is the brittle-to-ductile transition observed earlier [9,12] and is also shown in figure 2 of this report. In addition, Quach and Simha [18] observed a so-called glass-glass transition in polystyrene at 0.6kbar in their thermodynamic investigation. Certainly, the coincidence of such three transitions for the one polymer at similar pressure is noteworthy.

Results presented here infer that pressure appears to affect in opposition two major mechanisms; "void" suppression and fluid pumping. Pressure acts to reduce the "void" content in the polymer during deformation rendering craze initiation and growth more difficult. The second mechanism tends to increase the craze growth kinetics by providing an extremely high pressure gradient along the craze length. Such a pressure gradient will readily transport the viscous fluid to the craze tip.

A linear amorphous epoxy polymer was observed by Findly and Reed [19] to resist measurable hydrostatic creep up to 10,000 ksi (approximately 0.7kbar). That our polymer would tend to resist void suppression up to about 0.5kbar is reasonable. Thus, in regime I, the fluid pumping mechanism dominates resulting in craze growth enhancement and the consequent increase observed in the penetration coefficient. In regime I, there is competition between the two mechanisms (the pumping mechanism dominates) until at the transition pressure of 0.5kbar where the two mechanisms are believed to equalize. In regime II, the two mechanisms would continue to compete in a reverse order. At 3.0kbar, the deformation mechanism shifts from the dilational craze yielding to the nondilational shear yielding where no penetration was detected and the polymer undergoes the brittle-to-ductile transition. Interestingly enough the brittle-to-ductile transition of polystyrene exposed to

silicon oil was found to depend on the fluid viscosity [9].

4. Conclusions

Studies in tension and compression with polystyrene under superposed hydrostatic pressure using a silicon oil environment showed that a dilational component of the applied stress field is a necessary requirement for pressure-induced environmental stress cracking. Fourier transfer infrared spectroscopy was utilized for the first time in a semiquantitative study of the penetration kinetics of silicon oil into a solid polymer during deformation. Direct experimental evidence for the notion of a "dry" tip in environmental craze growth has been provided. These penetration studies proved that measurable amounts of silicon oil can penetrate only into preformed crazes, and that the concentration profile of the penetrant is closely related to the stress crazing and cracking effects.

Penetration of silicon oil into a cylinderical specimen has been modeled assuming fluid transport into porous media. An expression to describe the penetration kinetics has been developed which proved satisfactory when applied to the data. Pressure affects two opposing mechanisms; it acts to reduce the "void" content within the polymer which will make initiation and growth of crazes more difficult, and pressure tends to increase the craze growth rate by providing an extremely high pressure gradient along the craze length which is believed to drive the fluid to the craze tip. Due to these opposing two mechanisms the penetration behavior falls into two regimes with a transition at 0.5kbar.

ACKNOWLEDGEMENT

The authors wish to thank the Office of Naval Research for its generous financial support of this work.

References

1. G. A. Bernier and R. P. Kambour, Macromolecules, 1, 393 (1968).

2. G. P. Marshall, L. E. Culver and J. G. Williams, Proc. R. Soc. Lond. A., 319, 165 (1970).

3. E. H. Andrews and L. Bevan, Polymer, 13, 337 (1972).

4. I. Narisawa, J. Polym. Sci., A-2, 10, 1789 (1972).

5. R. P. Kambour, C. L. Gruner and E. E. Romagosa, J. Polym. Sci-Phys, 11, 1879 (1973).

6. E. J. Kramer and R. A. Bubeck, J. Polym. Sci-Phys,16, 1195 (1978).

7. H. A. Staurt, G. Markowski and D. Jaschke, Kunstoffe, 54, 618 (1964).

8. E. H. Andrews and J. M. Levy, Polymer, 15, 599 (1974).

9. K. Matsushige, S. Radcliffe and E. Baer, J. Macromol. Sci. Phys, B11, 565 (1975).

10. R. A. Duckett, B. C. Goswami, L. Stewart, I. M. Ward and A. M. Zihlif, Brit. Polym. J., 10, 11 (1978).

11. S. Rabinowitz, I. M. Ward and J. S. Parry, J. Mater. Sci., 5,29 (1970).

12. K. Matsushige, S. Radcliffe and E. Baer, J. Mater. Sci., 10, 833 (1975).

13. H. Ll. Pugh, ed. "High Pressure Engineering", Mech. Eng. Publications Ltd, London (1975).

14. W. J. Potts, Jr., "Chemical Infrared Spectroscopy", Wiley & Sons, New York (1963).

15. M. Hubert, J. Geology, 48, 785 (1940).

16. R. M. Barrer, Chapt. 6 in "Diffusion in Polymers, ed. by J. Crank and G. S. Park, Academic Press (1968).

17. J. Crank, "Mathematics of Diffusion", Oxford University Press, Fairlaw, New Jersey (1956).

18. A. Quach and R. Simha, J. Appl. Phys., 42, 4592 (1971).

19. W. N. Findly and R. M. Reed, Polym. Eng. Sci., 17, 837 (1977).

Figure captions

Figure 1: FTIR absorbance spectra of PS deformed in silicon oil, pure PS and the difference spectra, indicating bands at 1260cm^{-1} and 803 cm^{-1} characteristic of silicon oil.

Figure 2: The effect of pressure and silicon oil (500cSt) on the fracture stress (dotted lines) and yield stress (solid lines) of polystyrene in compression and in tension.

Figure 3: The effect of strain rate on the penetration of silicon oil (500cSt) into PS fractured in tension at atmospheric pressure.

Figure 4: The effect of strain level on silicon oil penetration into PS strained at atmospheric pressure for one hour.

Figure 5: Schematic representation of fluid penetration into preformed crazes started statistically from the surface of a large cylinder of radius α. r being the radius of dry core at time t.

Figure 6: Typical raidal concentration distribution of silicon oil (500cSt) penetrated into polystyrene at 1% constant strain for 30 minutes, 45 minutes and 85 minutes at atmospheric pressure. Solid lines are solutions of the penetration equation. Numbers on the curves are $\kappa t/\alpha^2$ values (see text).

Figure 7: The effect of additional unloaded soaking of polystyrene initially held at constant 1% strain under atmospheric pressure. Redistributions of oil due to additional soaking of one hour and 24 hours without load are also shown.

Figure 8: Nominal craze profile derived from silicon oil concentrations shown in figure 7. The distance OC represents the lag of the fluid front, C, behind the craze front, O.

Figure 9a: The effect of viscosity on the radial concentration distribution of various silicon oils penetrated into polystyrene at 1% strain for 1 hour under atmospheric pressure.

Figure 9b: The effect of silicon oil viscosity on the stress relaxation of polystyrene held at 1% strain under atmospheric pressure. Environmental relaxations are compared to "dry" relaxation of polystyrene in air.

Figure 10: Radial concentration distributions of silicon oil (500cSt) penetrated into polystyrene at 1% constant strain for various periods of time under 0.6kbar. Solid lines represent solutions of the penetration equation (see text).

Figure 11: Radial concentration distributions of silicon oil (500cSt) penetrated into polystyrene at 1% constant strain for various periods of time under 0.9kbar and 1.2kbar (inset). Solid lines are solution of the penetration equation. (see text)

Figure 12: The effect of pressure on the radial concentration distributions of silicon oil (500cSt) penetrated into polystyrene at 1% constant strain for one hour. Curves are fit of penetration equation to actual data. Numbers reported below the curves are values of $\kappa t/\alpha^2$. Corresponding pressures are reported above each curve.

Figure 13: Pressure dependence of silicon oil penetration coefficient, κ, into polystyrene ($-\log \kappa$) at 1% constant strain for one hour. Note the transition (arrow) at 0.5 kbar.

Table captions

Table 1: Penetration of silicon oil (500 cSt) into unloaded polystyrene.

Table 2: Penetration of silicon oil (500 cSt) into polystyrene under various loading conditions.

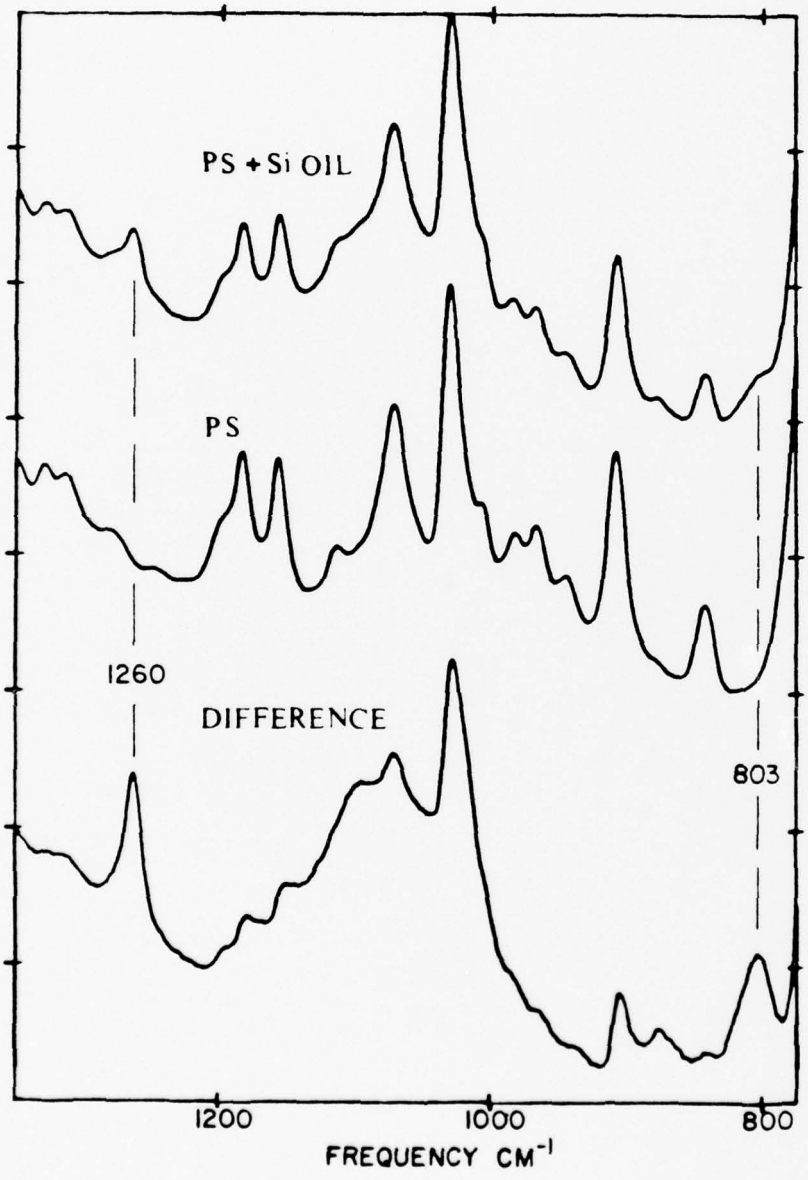

Figure 1

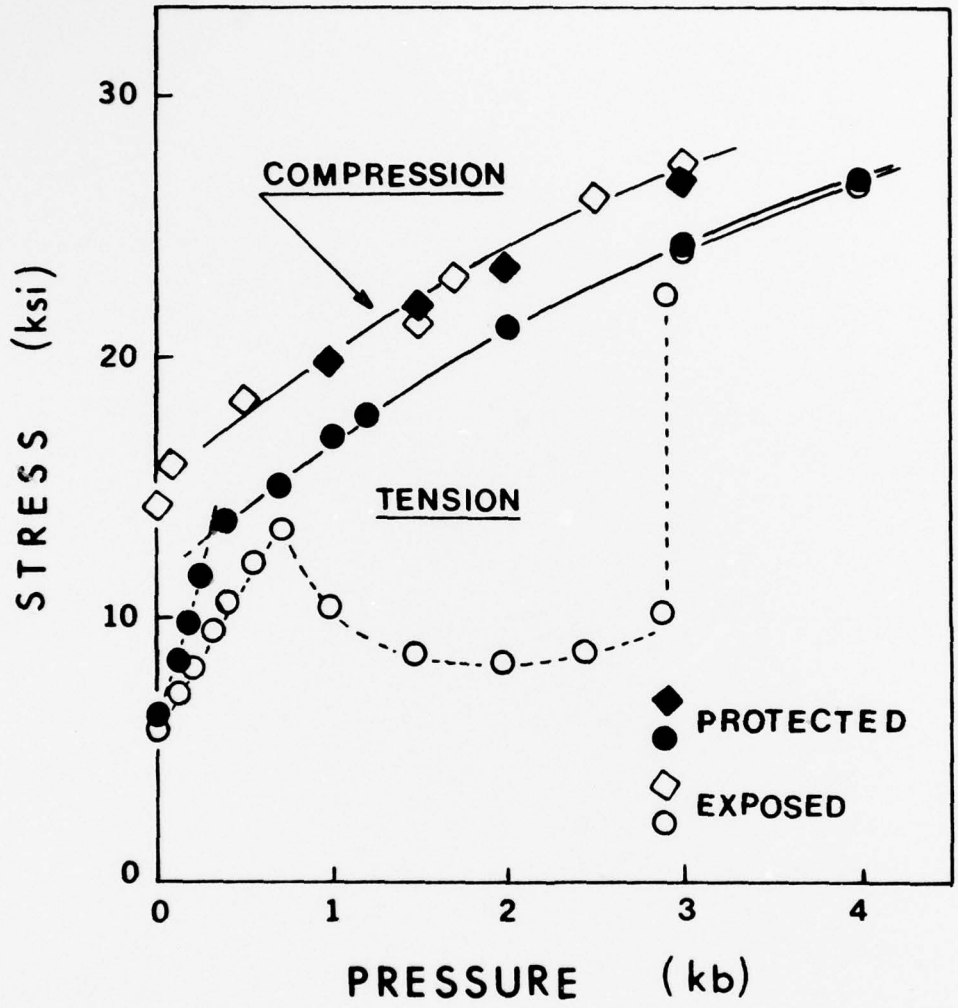
30
20
10
0
STRESS (ksi)
COMPRESSION
TENSION
PROTECTED
EXPOSED
0
1
2
3
4
PRESSURE (kb)

Figure 2

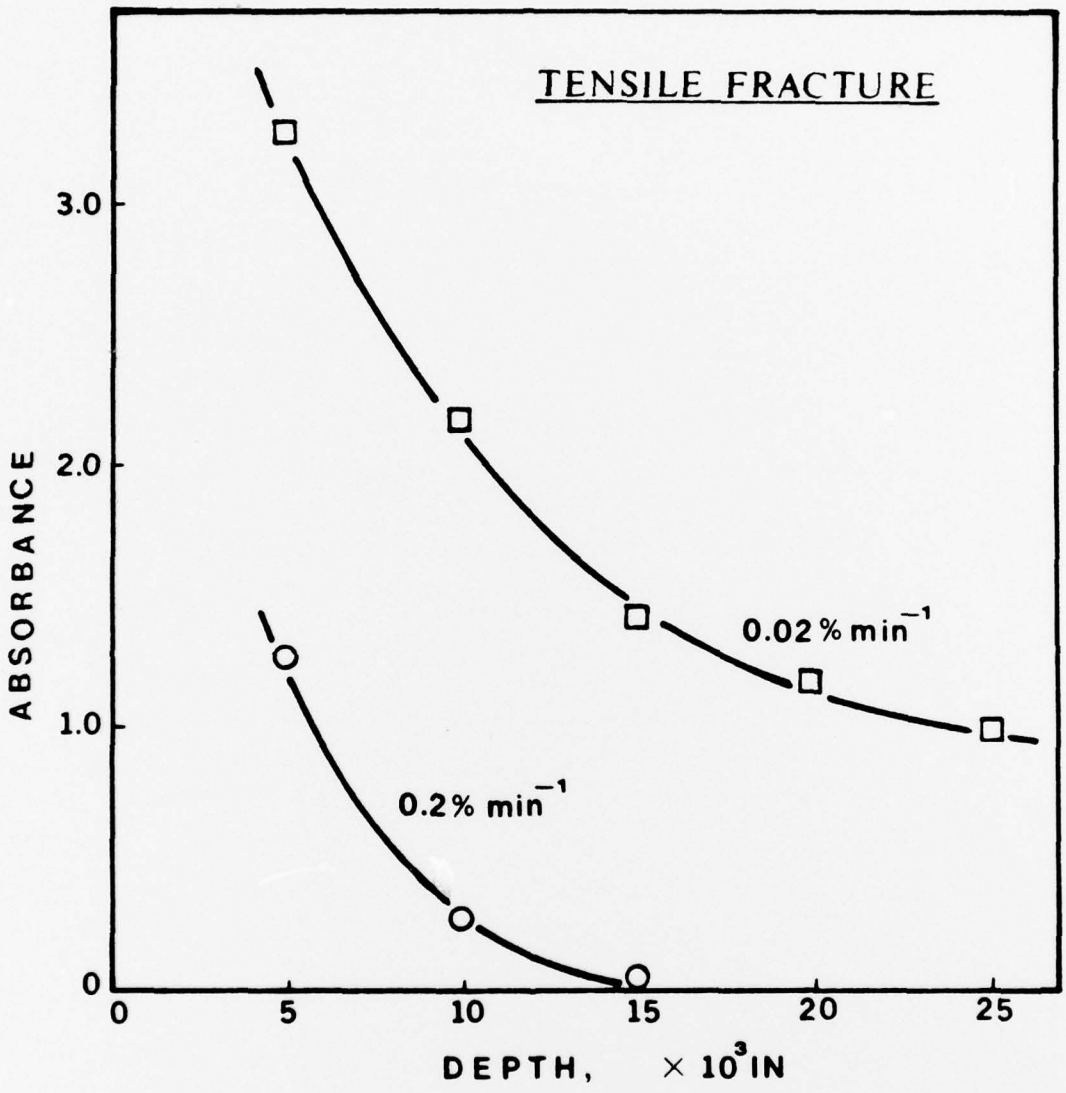
TENSILE FRACTURE
ABSORBANCE
3.0
2.0
1.0
0
0.02 % min⁻¹
0.2% min⁻¹
0
5
10
15
20
25
DEPTH, × 10³IN

Figure 3

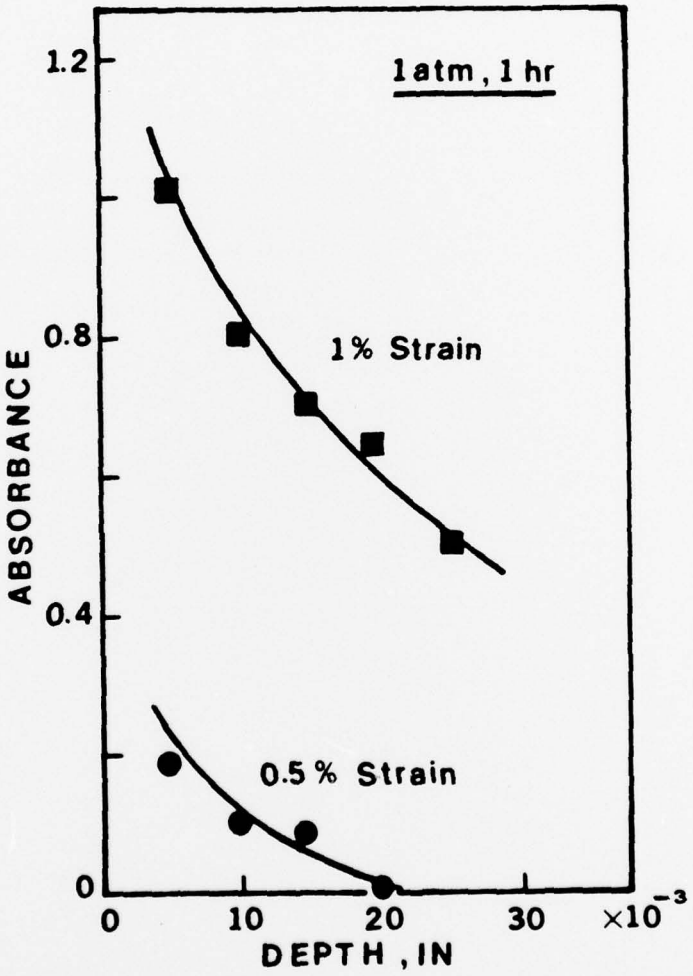
1 atm, 1 hr
1% Strain
0.5% Strain
ABSORBANCE
1.2
0.8
0.4
0
0
10
20
30
×10⁻³
DEPTH, IN

Figure 4

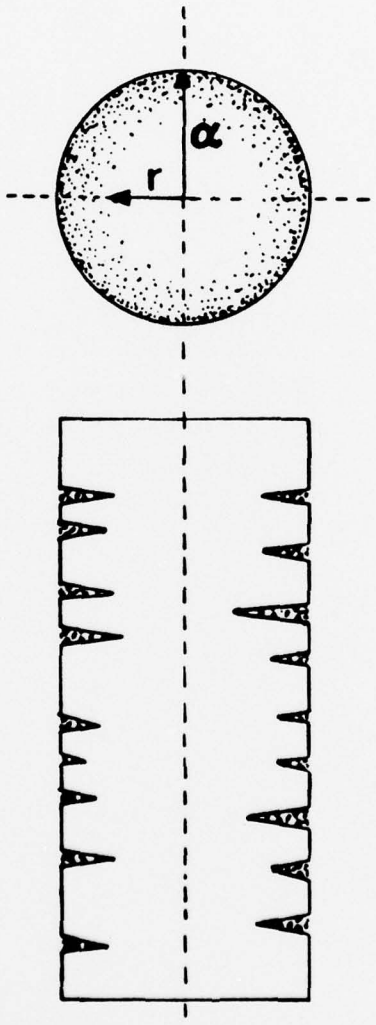

Figure 5

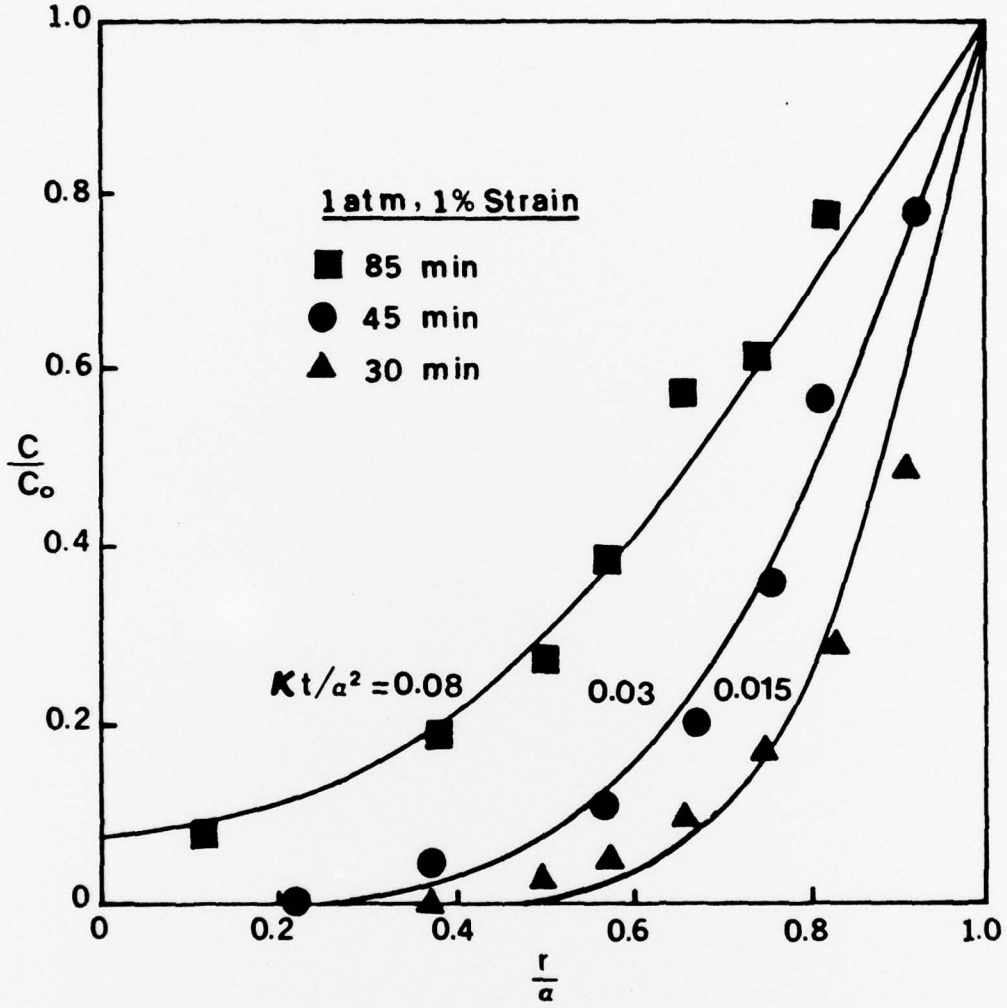
1 atm, 1% Strain
85 min
45 min
30 min
$Kt/a^2 = 0.08$
0.03
0.015
$\frac{C}{C_o}$
$\frac{r}{a}$
0
0.2
0.4
0.6
0.8
1.0

Figure 6

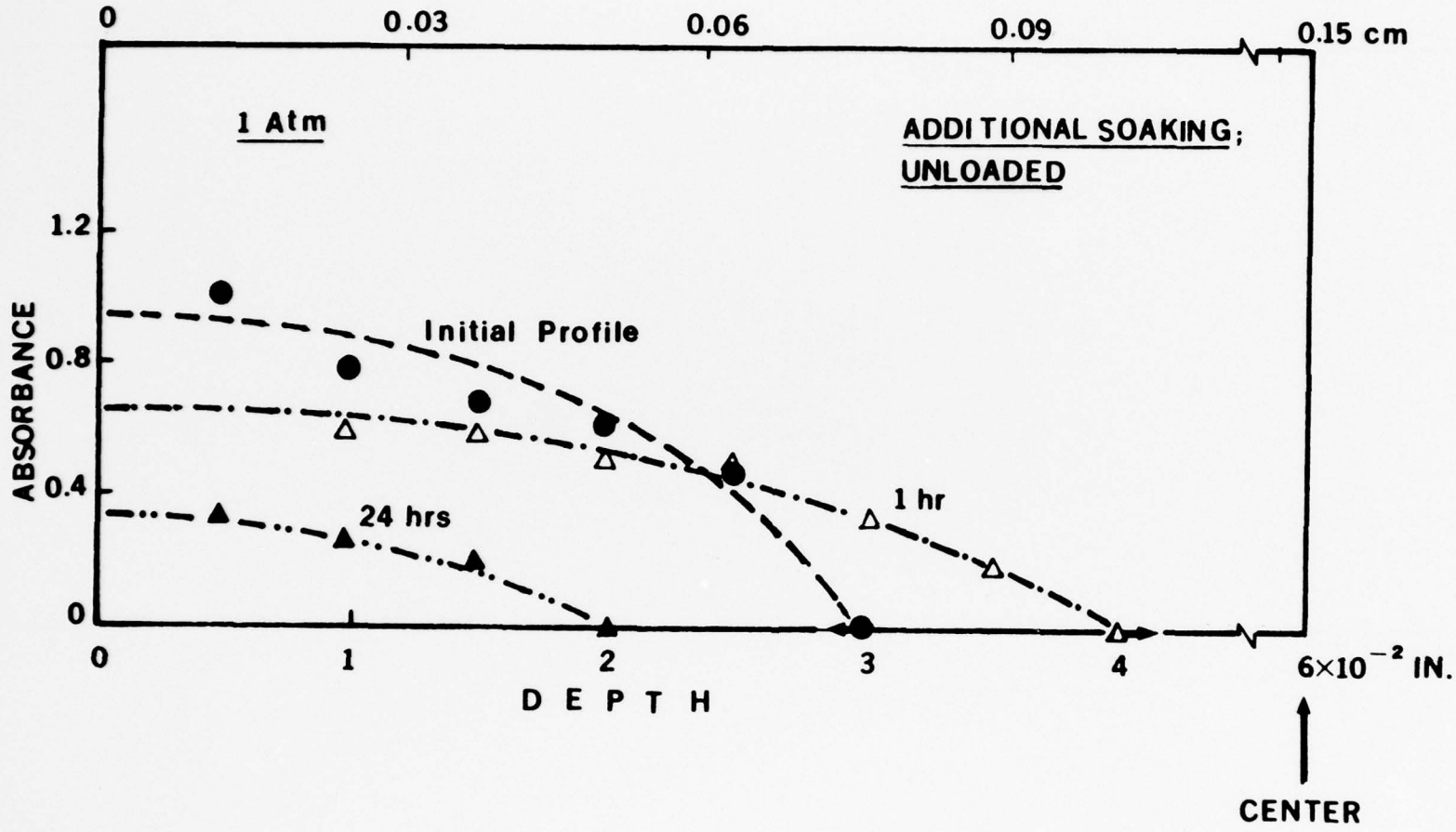
0
0.03
0.06
0.09
0.15 cm
1 Atm
ADDITIONAL SOAKING;
UNLOADED
1.2
0.8
0.4
0
ABSORBANCE
Initial Profile
1 hr
24 hrs
0
1
2
3
4
6×10⁻² IN.
D E P T H
CENTER

Figure 7

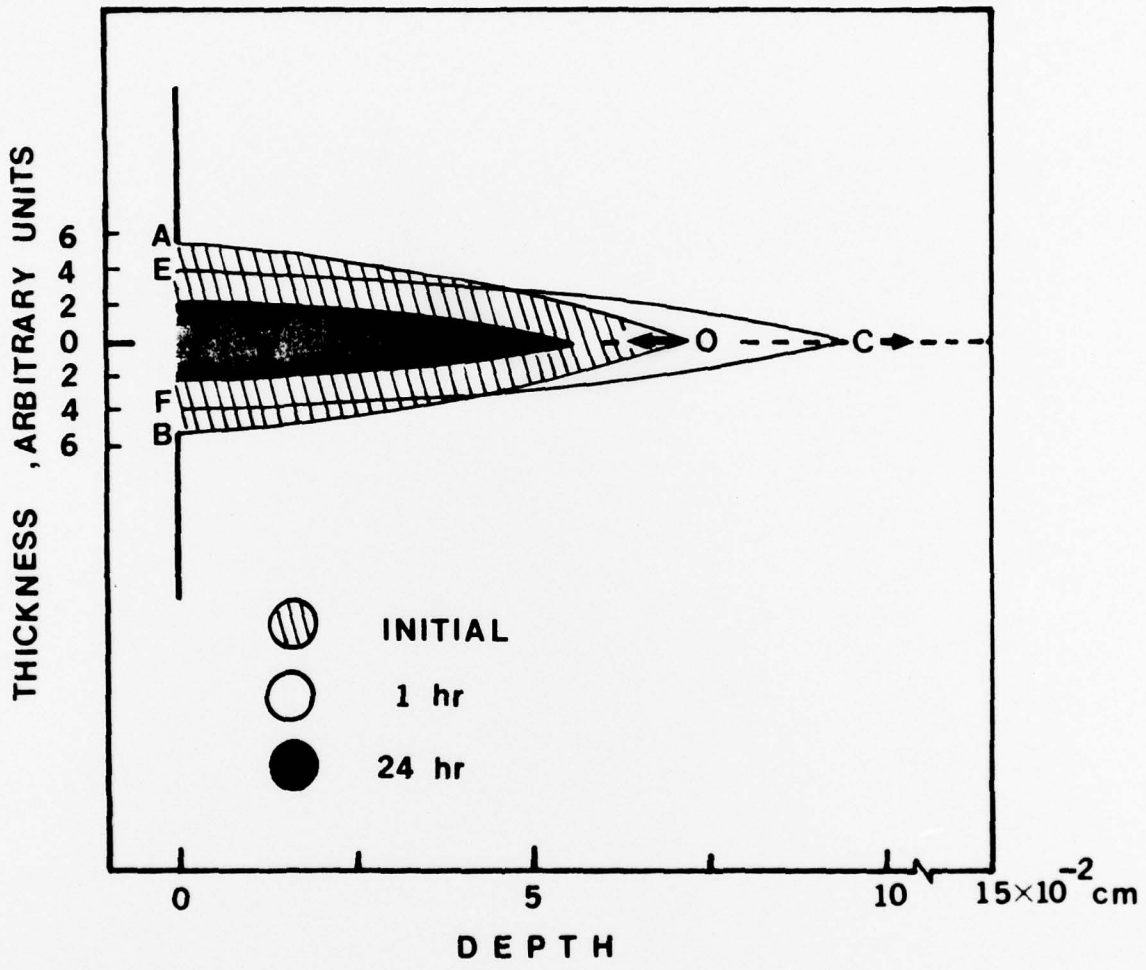
THICKNESS , ARBITRARY UNITS
6
4
2
0
2
4
6
A
E
F
B
O
C
INITIAL
1 hr
24 hr
0
5
10
15×10⁻² cm
DEPTH

Figure 8

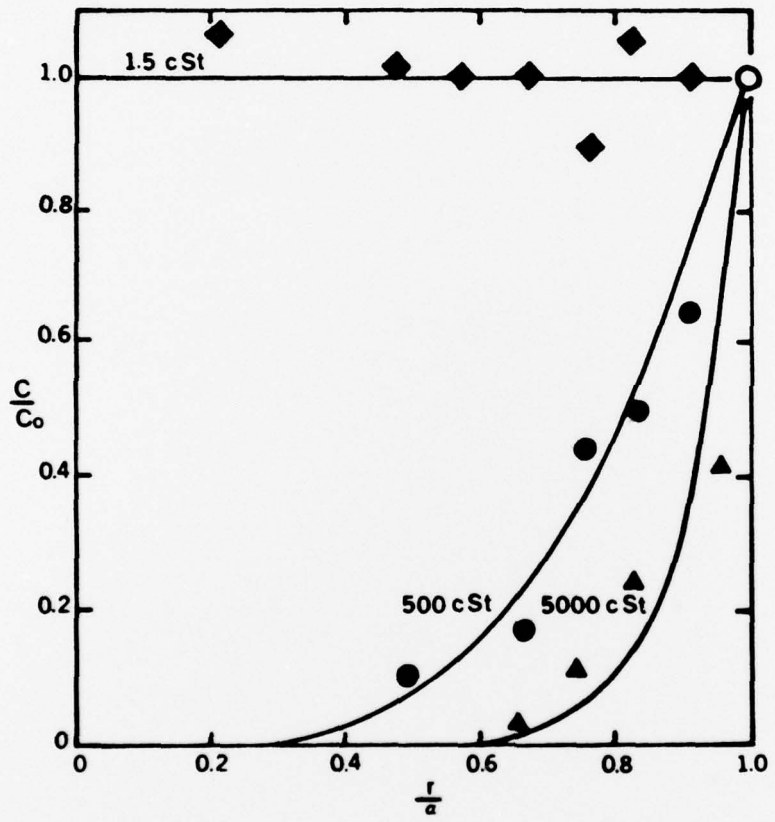

Figure 9a

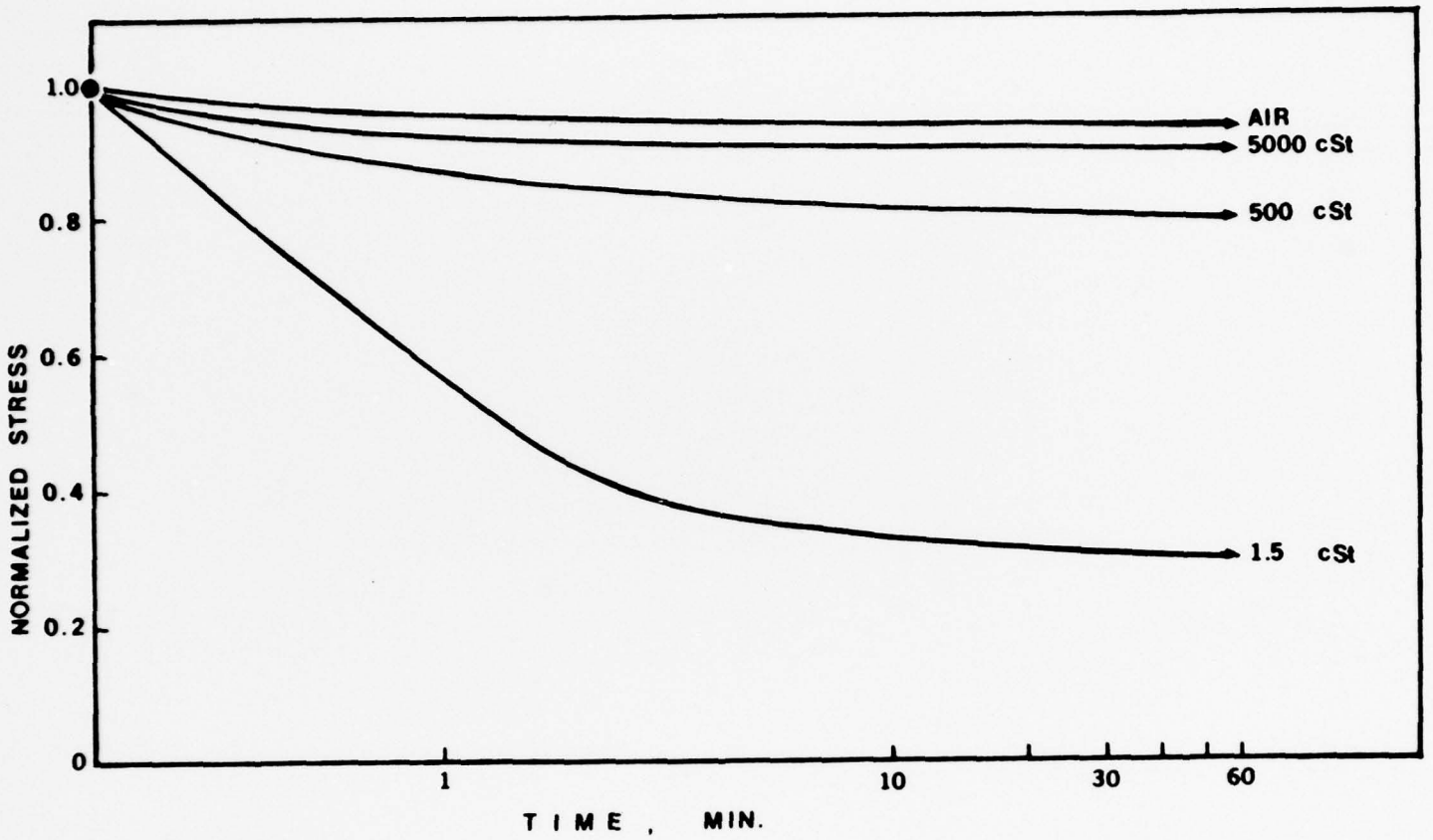
1.0
0.8
0.6
0.4
0.2
0
NORMALIZED STRESS
AIR
5000 cSt
500 cSt
1.5 cSt
1
10
30
60
TIME, MIN.

Figure 9b

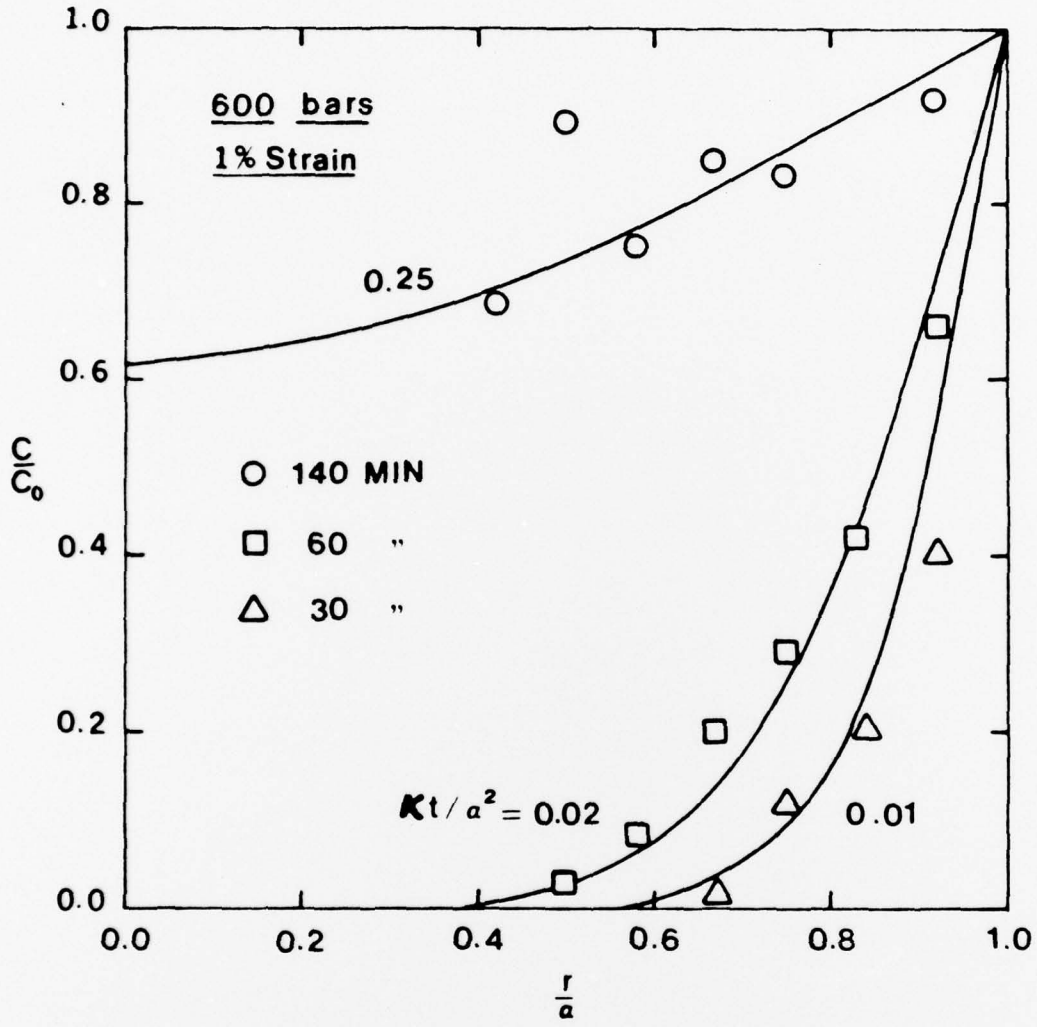
600 bars
1% Strain
0.25
140 MIN
60 "
30 "
$Kt/a^2 = 0.02$
0.01
$\frac{C}{C_0}$
$\frac{r}{a}$
0.0
0.2
0.4
0.6
0.8
1.0

Figure 10

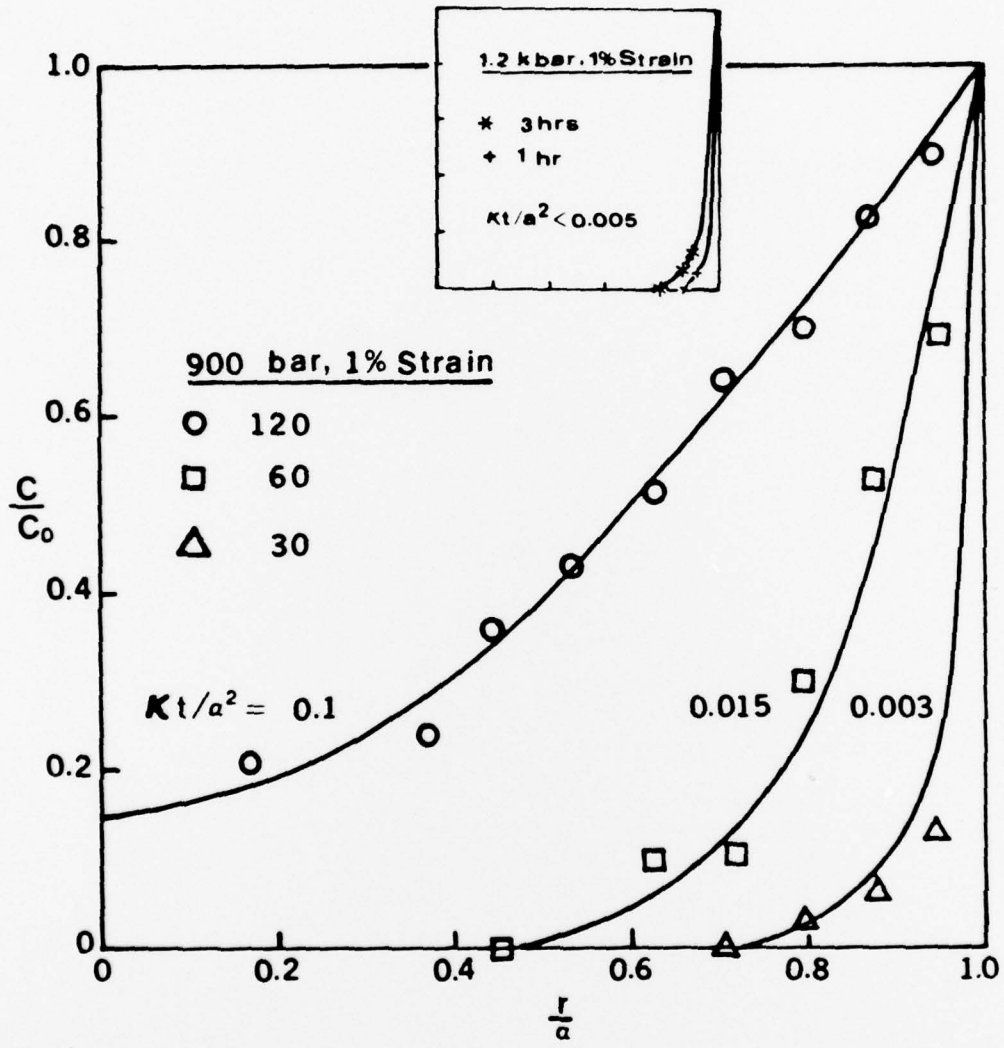
1.2 k bar, 1% Strain
* 3 hrs
+ 1 hr
Kt/a² < 0.005
900 bar, 1% Strain
120
60
30
Kt/a² = 0.1
0.015
0.003
C/C₀
r/a
0
0.2
0.4
0.6
0.8
1.0

Figure 11

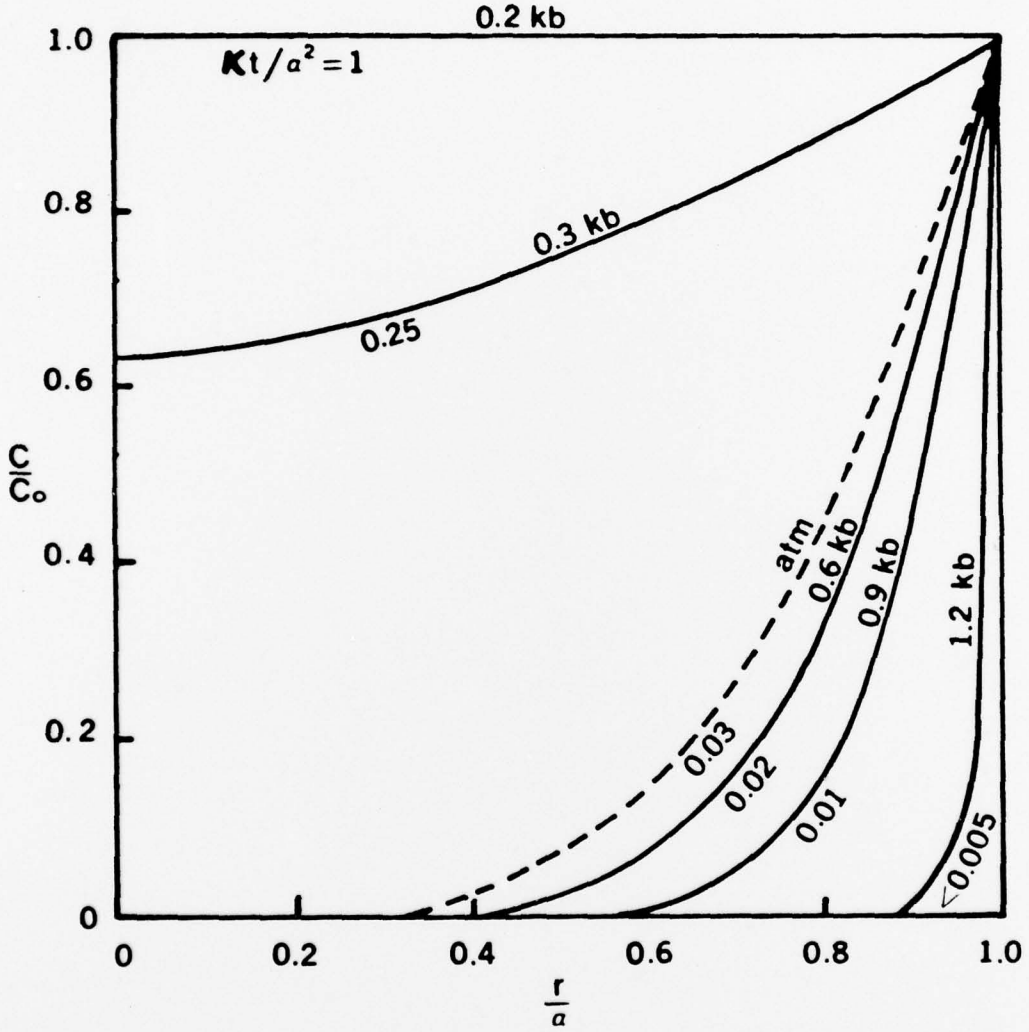
0.2 kb
$Kt/a^2 = 1$
0.3 kb
0.25
atm
0.6 kb
0.9 kb
1.2 kb
0.03
0.02
0.01
0.005
1.0
0.8
0.6
0.4
0.2
0
$\frac{C}{C_o}$
0
0.2
0.4
0.6
0.8
1.0
$\frac{r}{a}$

Figure 12

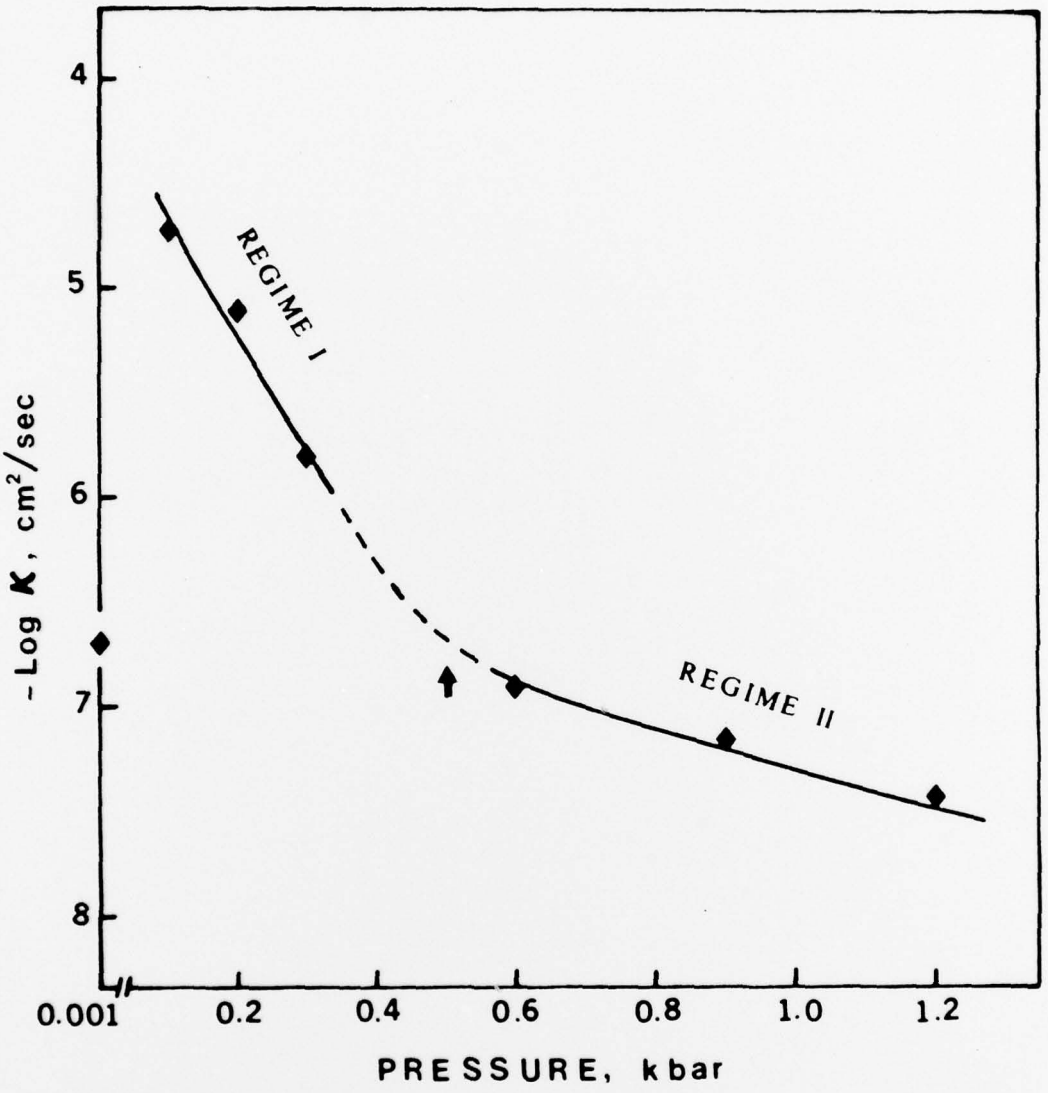
4
5
6
7
8
-Log K, cm²/sec
REGIME I
REGIME II
0.001
0.2
0.4
0.6
0.8
1.0
1.2
PRESSURE, kbar

Figure 13

Table 1

Soaking Condition	Soaking time (hr.)	Depth X 10^3, inches					
		5	10	15	20	25	30
As it is	5760	0	0	0	0	-	-
Crazed*	0.5	0.758	0.338	0.230	0.209	0.058	0
At 1.0 Kbar**	2	0.	0	0	0	-	-

*Sampled was precrazed for 4 hours at 1% strain in air then immediately soaked in silicon oil.

**Only hydrostatic pressure, no tension was applied.

Table 2

Pressure (bars)	Strain %	Time (minutes)	5	10	15	20	25	30
4K	None	120	0	0	0	0	-	-
4K	3.5 (Shear Banding)	60	0	0	0	-	-	-
1	1 (Crazing	30	0.68	0.44	0.26	0.18	0.13	-
100	1 (Crazing)	30	2.31	2.41	2.41	2.29	2.42	2.20*
100	-3 (Compression)	30	0	0	0	-	-	-

*Silicon oil penetration continued at an average level of 2.3 absorbance units, all the way to the center.